High Temp. Mater. Proc., Vol. **31** (2012), pp. 157–162 DOI 10.1515/htmp-2011-0157

Single-Source Molecular Precursor for Synthesis of CdS Nanoparticles and Nanoflowers

Masoud Salavati-Niasari[1,2,*] **and Azam Sobhani**[2]

[1] Institute of Nano Science and Nano Technology, University of Kashan, Kashan, I.R. Iran

[2] Department of Inorganic Chemistry, Faculty of Chemistry, University of Kashan, Kashan, I.R. Iran

Abstract. CdS Semiconductor nanostructures were synthesized by using two different methods. Using triphenylphosphine ($C_{18}H_{15}P$) and oleylamine ($C_{18}H_{37}N$) as surfactant, CdS semiconductor nanocrystals with a size ranging from 30 to 90 nm can be synthesized by thermal decomposition of precursor [bis(thiosemicarbazide)cadmium(II)]. CdS nanoflowers were synthesized via hydrothermal decomposition of [bis(thiosemicarbazide) cadmium(II)] without any surfactant. X-ray diffraction (XRD) patterns confirm that the resulting samples were a pure hexagonal phase of CdS. The optical property test indicates that the absorption peak of the samples shifts towards short wavelength, and the blue shift phenomenon might be ascribed to the quantum effect.

Keywords. Nanoparticles, thermal decomposition, hydrothermal, cadmium sulfide, optical property.

PACS®(2010). 61.46.-w, 61.46.Df, 61.46.Hk, 65.80.+n, 78.66.-w, 78.66.Hf, 78.67.-n, 78.67.Bf, 81.07.-b, 81.07.Bc, 81.16.-c, 81.16.Be.

1 Introduction

Nanotechnology develops stormy last 20 years and finds new areas of application. Nanocrystalline semiconductor quantum dots have been intensively investigated during the last decade [1–6]. Their optical, electronic, and catalytic properties can be basically attributed to two factors, i.e. the large surface to volume ratio and the size quantization effect, both leading to alterations of the semiconductor properties. Size, morphology and dimensionality can strongly affect the properties of nanostructured materials. Cadmium sulfide (CdS) is a kind of attractive semiconductor material, and it is now widely used for optoelectronic applications such as non-linear optical devices and flat panel displays, light emitting diodes (LED), lasers, thin film transistors, photosensitive resistance, electric eye, and so forth [7–10].

Sized-controlled inorganic nanoparticles such as metals, semiconductors, and metal oxide have attracted more interests because of their material properties compared with their bulk. Hence, investigations on the synthesis and modification of nanosized CdS have attracted tremendous attentions. A variety of methods have been developed to prepare the sulfides of zinc and cadmium, including solid phase reaction [11], gas phase reaction with H_2S or sulfur vapor [12], sol-gel process [13], hydrothermal or solvothermal route [14–16] and gamma-irradiation technique [17, 18]. CdS with particular structures like quantum dots [19, 20], nanowires [21, 22], nanoporous particles [23], hollow submicrospheres [24], and so on have been successfully synthesized. Recently, our group reported synthesis of CdS nancrystallits via hydrothermal process [25, 26]. This method has been also reported to prepare metal selenide [27] and telluride [28] nanostructures. In present work CdS nanoparticles have been prepared by a thermal decomposition route from $[Cd(TSC)_2]Cl_2$ (TSC = thiosemicarbazide) as single precursor. The use of thiosemicarbazide complexes as precursors seems to be interesting, because at the thermal decomposition of these complexes existing Cd–S bond and its environment is "inherited". The use of thiosemicarbazide complexes of different structure allows controlling the structure of obtained semiconductor materials [29].

2 Experimental

2.1 Materials and Physical Measurements

Oleylamine, triphenylphosphine (TPP), hexane, toluene and absolute ethanol were purchased from Aldrich and used as received. The XRD pattern of products was recorded by a Rigaku D-max C III XRD using Ni-filtered Cu Kα radiation. Elemental analyses were obtained on a Carlo ERBA Model EA 1108 analyzer. Scanning electron microscopy (SEM) images were obtained on Philips XL-30ESEM equipped with an energy dispersive X-ray spectroscopy. Transmission electron microscopy (TEM) images were obtained on a Philips EM208 transmission electron microscope with an accelerating voltage of 100 kV. Fourier

* **Corresponding author:** Masoud Salavati-Niasari, Institute of Nano Science and Nano Technology, University of Kashan, Kashan, P. O. Box. 87317–51167, I.R. Iran; E-mail: salavati@kashanu.ac.ir.

Received: August 13, 2011. Accepted: December 20, 2011.

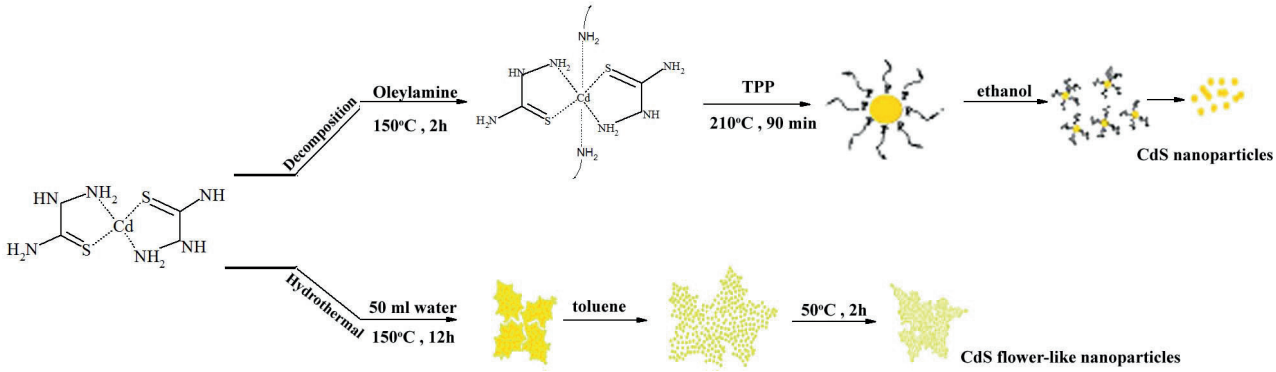

Scheme 1. Proposed mechanism for preparation of CdS nanoparticles by two methods.

transform infrared (FT-IR) spectra were recorded on Shimadzu Varian 4300 spectrophotometer in KBr pellets. The room temperature PL was studied on an F-4500 fluorescence spectrophotometer.

2.2 Synthesis of $[Cd(TSC)_2]Cl_2$ Complex

Cadmium(II) chloride monohydrate $CdCl_2 \cdot H_2O$, 2 mmol, was dissolved in 20 ml distilled water, a solution of thiosemicarbazide ($H_2NNHCSNH_2$), 4 mmol, dissolved in 50 mL of distilled water containing 37% hydrochloric acid was dropwise added into the above solution under magnetic stirring. After addition of all the reagents, the mixture was refluxed for about 6 h with evaporation of the solution; a white crystalline solid was recovered. It was filtered, washed with distilled water and ethanol and dried. We suppose that thiosemicarbazide is coordinated to cadmium ion as bidentate cyclic ligand through the S atom and the terminal N atom of the hydrazine fragment. Since cadmium (II) being d^{10} ion usually adopts a coordination number four with tetrahedral stereochemistry, it may be presumed that the ligand in this metal complex has been arranged in a tetrahedral manner. IR (KBr) ν_{max} cm^{-1}: 3267 $\nu_{as}(NH_2)$, 3231 $\nu_s(NH_2)$, 3175 ν(NH), 1148 ν(C-N), 790 ν(C=S), 411 ν(M-S), 364 ν(M-N). Anal. Calcd. for $[Cd(TSC)_2]Cl_2$: C, 6.57; H, 2.76; N, 22.99; S, 17.54; Cd, 30.75. Found: C, 6.49; H, 2.90; N, 23.17; S, 17.42; Cd, 30.80% [30–36].

2.3 Preparation of CdS Nanoparticles

In the current synthetic procedure that have been shown in Scheme 1, first, 0.6 g $[Cd(TSC)_2]Cl_2$ and 5 mL oleylamine loaded in a 50 ml two-neck distillation were heated up to 150 °C for 120 min and a light yellow solution was generated with the gradual dissolution of precursor complex $[Cd(TSC)_2]Cl_2$. Then, 5 g of TPP was dissolved in the mixture. The solution was aged at 210 °C for 90 min. The color of the solution changed from yellow to orange, indicating that colloidal nanoparticles were generated. The thermal decomposition of the thiosemicarbazide complex at 210 °C led to a formation of CdS nanoparticles. The nanoparticles were precipitated by adding excess ethanol to the solution. The yellow precipitate was collected via centrifugation after 15 min of stirring. The nanoparticles could easily be re-dispersed in nonpolar organic solvents, such as hexane or toluene. This synthetic procedure is a modified version of the method developed by Hyeon and co-workers for the synthesis of nanocrystals of metals that employs the thermal decomposition of transition metal complexes [37].

2.4 Preparation of Flower-like CdS Nanoparticles

Nanoflower of CdS were synthesized according to this procedure: 0.8 g of the $[Cd(TSC)_2]Cl_2$ dissolved in 50 mL of distilled water, was put into a Teflon-lined stainless steel autoclave of 100 ml capacity. The autoclave was sealed and maintained at 150 °C for 12 h, then allowed to cool to room temperature naturally. The yellow solid formed was separated by centrifugation and re-dissolved in toluene for further analysis. The nanoflowers dried in vacuum at 50 °C for 2 h. In the current synthetic procedure that have been shown in Scheme 1. The yield of the overall synthesis was 81% based on the amount of $[Cd(TSC)_2]Cl_2$.

3 Results and Discussion

Figure 1 shows the XRD patterns of the CdS nanoparticles and CdS nanoflowers. All of the reflections of the XRD pattern in Figure 1 (a) can be indexed to the standard pattern of the pure hexagonal phase of CdS which is in good agreement with the reported data (space group: $P63mc$; JCPDS No. 77-2306) and lattice constants $a = 0.4136$, $b = 0.4136$ nm and $c = 0.6713$ nm. No diffraction peaks from other crystalline forms are detected, which indicates a high purity of these CdS samples. In addition, the intense and sharp diffraction peaks suggest that the obtained product is well crystallized. From XRD data, the crystallite size (D_c) of as-prepared CdS particles was calculated to be 40

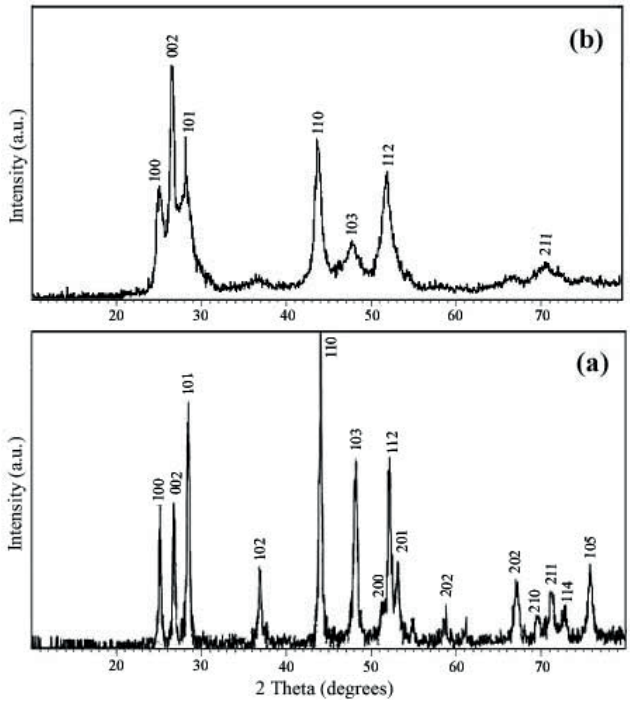

Figure 1. XRD patterns of (a) CdS nanoparticles and (b) CdS nanoflowers.

nm using the Debey–Scherrer equation (1) [38],

$$D_c = \frac{K\lambda}{\beta \cos\theta}, \tag{1}$$

where β is the width of the observed diffraction line at its half-intensity maximum, K is the so-called shape factor, which usually takes a value of about 0.9, and λ is the wavelength of X-ray source used in XRD.

Figure 1 (b) is the X-ray powder diffraction pattern of the flower-like CdS nanoparticles showing reflections from (100), (002) and (101) planes, which indicates formation of a pure hexagonal phase which is very close to the values in the literature (JSPDS No.41-1049). The crystallite size estimated from the Scherrer formula, is about 21 nm.

The elemental composition of the CdS nanoparticles is determined by energy dispersive spectrometry, which displays cadmium Lα_1 (3.18 KeV), Lβ_1 (3.51 KeV), and Lβ_2 (3.73 KeV) peaks and sulfur Kα_1 (2.35 KeV) peaks.

The morphology and structure of the as-prepared CdS nanopowders were investigated by SEM and TEM images. The SEM analysis images (Figure 2) show that the powders have granular morphology. In order to further elucidate the size and the crystal structure of the nanoparticles, TEM image was taken (Figure 2). The morphology of particles is close to regular spherical and their distribution is not uniform (30–90 nm).

Figure 3 reveals the SEM images of the 5 CdS flower-like nanoparticles prepared at 150 °C by hydrothermal method. Figure 3 (a) shows that the individual CdS flower is composed of several flowers that are collected and have petals. Interesting phenomenon is that each petal consists of some non-smooth nanospheres. Similar phenomena are also found toward the other individual CdS flowers. These findings also can be seen in Figure 3 (b) with higher magnification. TEM images of products have been shown in Figures 3 (c) and (d). The panoramic view with low magnification in Figure 3 (c) demonstrates that products are near to spheres and exist with a diameter of 30–90 nm. Further observation based on the high magnification image (Figure 3 (d)) shows in fact the spheres are flowers with average diameter of about 30 nm that collected and formed a big flower.

To investigate whether the surface of the nanoparticles was capped with organic surface, FT-IR of the as-synthesized samples was performed. Figure 4 shows the FT-IR spectrum of CdS nanoparticles. Since CdS has no absorption peaks in the range of 500–4000 cm^{-1}, the peaks at 2921 and 2869 cm^{-1} are due to the symmetric and asymmetric CH_2 stretching modes, the peak at 3010 cm^{-1} is due to the n(C–H) mode of the C–H bond adjacent to the C=C bond, and the small peak at 1625 cm^{-1} is due to the n(C=C) stretching mode. In addition, the peak at 1460 cm^{-1} is due to the NH_2 scissoring mode. The results clearly reveal that the nanoparticles are coated with small amount of the oleylamine [39–41]. FT-IR spectrum of CdS flower-like nanoparticles are the same as the presented spectra.

Figures 5 (a) and (b) shows photoluminescence (PL) spectra of CdS nanoparticles prepared via thermal decomposition and hydrothermal method, respectively. The PL spectrum of the CdS nanoparticles shows an emission maximum at 461 nm (λ_{exc} = 340 nm) (Figure 5 (a)) and an emission maximum for CdS flower-like at 430 nm (λ_{exc} = 342 nm) (Figure 5 (b)). Previous reports suggest that the emission arises from the recombination of an electron trapped in a sulfur vacancy with a hole in the valence band of CdS [42]. As the crystallite size decreases, intensity of emission peak increases and the peak shifts to higher frequencies that indicating quantum confinement effect [43,44]. The PL shows a blue shift with respect to bulk CdS (512 nm, 2.4 eV) [42]. This emission spectra of CdS nanoparticles obtained by decomposition, as calculated by the direct band gap method [43], is 461 nm (2.69 eV), showing a blue shift of 51 nm in relation to that of the bulk material. The emission spectra calculated at 430 nm (2.88 eV) shows a blue shift in relation to the bulk material.

Thermal decomposition of the precursor complex at 210 °C with formation of finely dispersed cadmium sulfides and elimination of gaseous products (Eq. (2)):

$$[Cd(H_2NNHCSNH_2)_2] \xrightarrow{210\,^{\circ}C,\ air} CdS + 3N_2\uparrow + H_2S\uparrow + 2CO_2\uparrow + 4H_2O\uparrow.$$

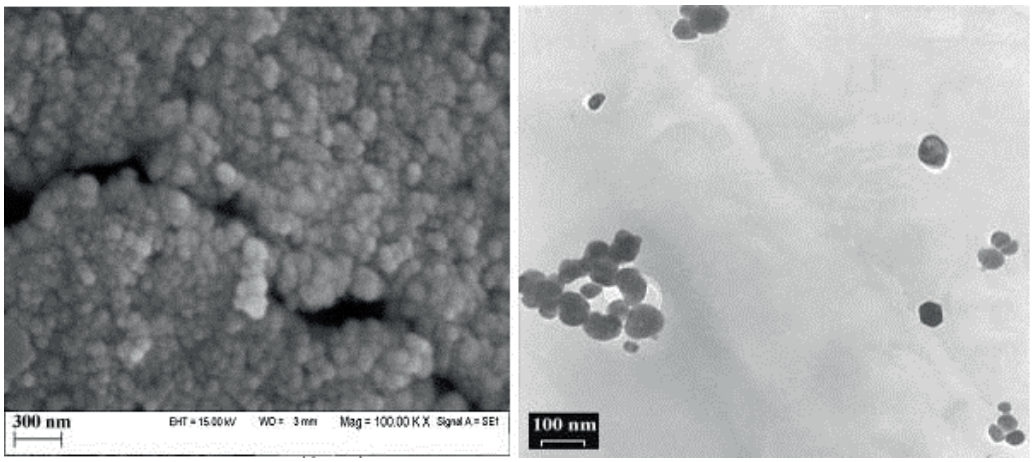

Figure 2. SEM and TEM image of CdS nanoparticles.

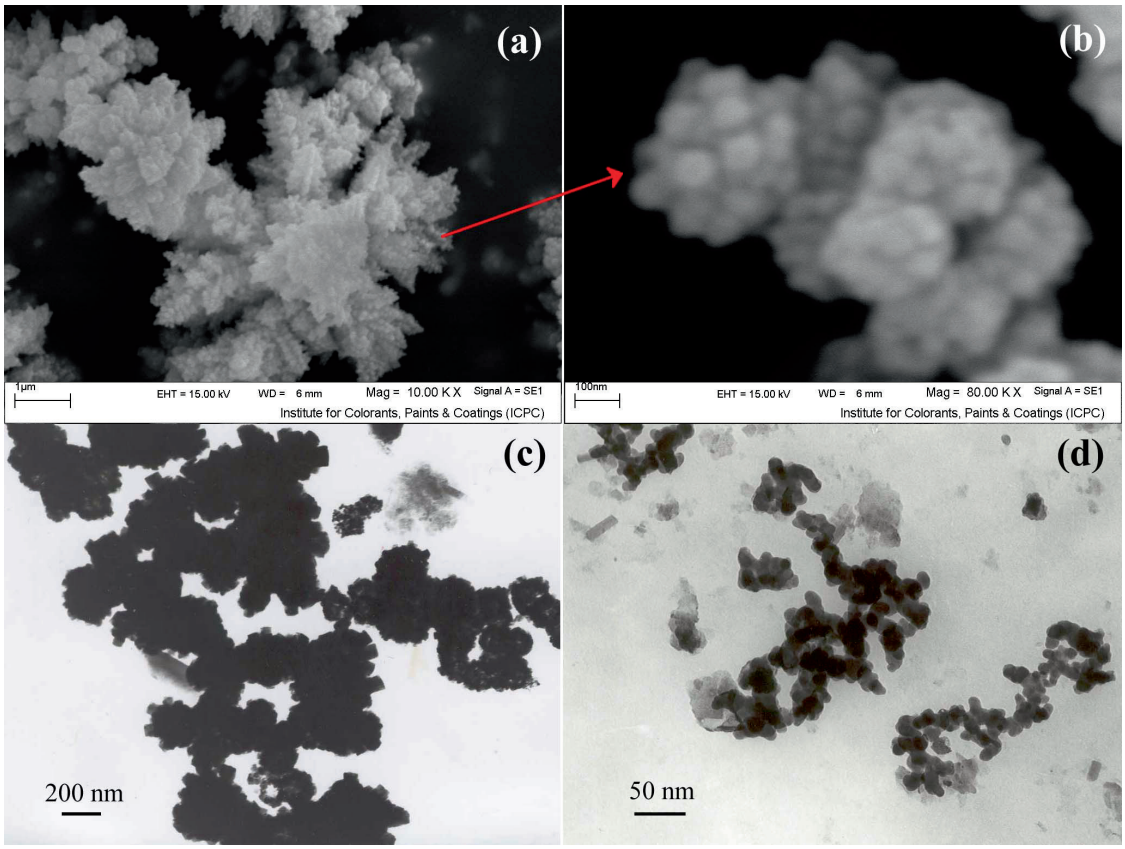

Figure 3. (a), (b) SEM and (c), (d) TEM images of CdS flower-like nanoparticles.

During thermal decomposition reaction, nucleation rate for nanocrystals could reach a high value in a short time and these nuclei were wrapped by surfactant. Consequently, the formed nanocrystals grow to a certain value and saturate. The effect of the surfactant is to control the size of the particles and to prevent the aggregation of particles. When the concentration of the surfactant is low, the nuclei can not be wrapped by the surfactant completely; wide size distribution of nanocrystals was obtained. Oleylamine is known as a ligand that binds tightly to the nanoparticles surface. TPP is a high-boiling point surfactant with a patulous long-chain structure providing greater steric hindrance. The ad-

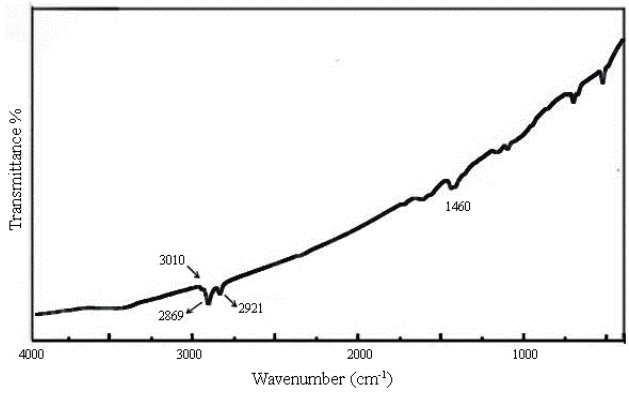

Figure 4. FT-IR spectrum of the CdS nanoparticles synthesized via decomposition of precursor.

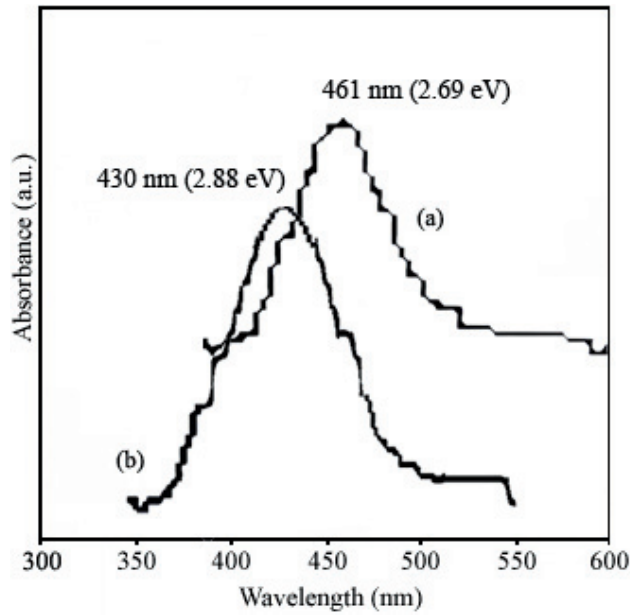

Figure 5. PL spectra of the prepared: (a) CdS nanoparticles via decomposition of precursor and (b) CdS flower-like nanoparticles via hydrothermal method.

dition of TPP into the mixture of oleylamine and complex as an additional surfactant led the particles to be well dispersed.

4 Conclusions

In summary, CdS semiconductor nanocrystals have been synthesized by two simple approach: thermal decomposition of [bis(thiosemicarbazide)cadmium(II)] and hydrothermal method. These reaction routes can further be applied to prepare other metal sulfides. The results obtained with XRD of CdS nanoparticles show that our experimental methodology produces nanoparticles predominantly grown in a hexagonal lattice. This nanoparticles have a size ranging from 30 to 90 nm and their morphology is close to regular spherical. PL energy of CdS Nanoparticles is blue shifted in comparison with the band gap of bulk CdS that indicating formation nanoparticles.

Acknowledgments

Authors are grateful to the council of university of Kashan for their unending effort to provide financial support to undertake this work.

References

[1] P. V. Kamat, K. Murakoshi, Y. Wada, S. Yanagida, in: H. S. Nalwa (Ed.), Handbook of Nanostructured Materials and Nanotechnology, Academic Press, San Diego, 2000, p. 129.
[2] T. Trindade, P. O' Brien, N. L. Pickett, Chem. Mater. 13 (2001), 3843–3858.
[3] L. Brus, J. Phys. Chem. Solids 59 (4) (1998), 459–465.
[4] A. P. Alivisatos, J. Phys. Chem. 100 (31) (1996), 13226–13229.
[5] H. Weller, Angew. Chem. 32 (1993), 41–53.
[6] A. Henglein, Chem. Rev. 89 (1989), 1861–1873.
[7] X. F. Duan, Y. Huang, R. Agarwal, C. M. Lieber, Nature 421 (2003), 241–245.
[8] Y. K. Liu, J. A. Zapien, C. Y. Geng, Y. Y. Shan, C. S. Lee, S. T. Lee, Appl. Phys. Lett. 85 (2004), 3241–3243.
[9] S. Kar, B. Satpati, P. V. Satyam, S. Chaudhuri, J. Phys. Chem. B 109 (2005), 19134–19138.
[10] Y. W. Jun, S. M. Lee, J. Cheon, J. Am. Chem. Soc. 123 (2001), 5150–5151.
[11] W. Wang, Z. Liu, C. Zheng, C. Xu, Y. Liu, G. Wang, Mater. Lettr, 57 (2003), 2755–2760.
[12] M. Abboudi, A. Mosset, J. Solid State Chem. 109 (1994) 70–73.
[13] V. I. Boev, A. Soloviev, B. Rodríguez-González, C. J. R. Silva, M. J. M. Gomes, Mater. Lett. 60 (2006), 3793–3796.
[14] W. Qingqing, X. Gang, H. Gaorong, J. Solid State Chem. 178 (2005), 2680–2685.
[15] H. Zhang, D. Yang, X. Ma, D. Que, Mater Lett. 59 (2005), 3037–3041.
[16] U. K. Gautam, R. Seshadri, C. N. R. Rao, Chem. Phys. Lett. 375 (2003), 560–564.
[17] A. Chatterjee, A. Priyam, S. K. Das, A. Saha, J. Colloid Interface Sci. 294 (2006), 334–342.
[18] Y. Ni, X. Ge, Z. Zhang, Mater. Sci. Eng. B 130 (2006) 61–65.
[19] Q.-H. Zhong, C.-H. Liu, Thin Solid Films, 516 (2008), 3405–3410.
[20] Z. A. Peng, X. G. Peng, J. Am. Chem. Soc. 123 (2001) 183–184.
[21] Y. Wang, L. Zhang, C. Liang, G. Wang, X. Peng, Chem. Phys. Lett. 357 (2002), 314–318.
[22] D. Xu, Z. P. Liu, J. B. Liang, Y. T. Qian, J. Phys. Chem. B 109 (2005), 14344–14349.
[23] J. S. Hu, L. L. Ren, Y. G. Guo, H. P. Ling, A. M. Cao, L. J. Wan, C. L. Bai, Angew. Chem., Int. Ed. 44 (2005), 1269–1273.

[24] J. Huang, Y. Xie, B. Li, Y. Liu, Y. T. Qian, Adv. Mater. 12 (2000), 11–14.

[25] M. Salavati-Niasari, F. Davar, M. Loghman-Estarki, J. Alloys Comp. 481 (2009), 776–780.

[26] M. Salavati-Niasari, M. Loghman-Estarki, F. Davar, Chem. Eng. J. 145 (2008), 346–350.

[27] A. Sobhani, F. Davar, M. Salavati-Niasari, Appl. Sur. Sci. 257 (2011), 7982–7987.

[28] M. Salavati-Niasari, M. Bazarganipour, F. Davar, J. Alloys Compd. 489 (2010), 530–534.

[29] M. Salavati-Niasari, A. Sobhani, F. Davar, J. Alloys Compd. 507 (2010), 77–83.

[30] E. Larsen, P. Trinderup, Acta Chem. Scand. A. 29 (1975) 481–483.

[31] D. S. Mahadevappa, A. S. A. Murthy, Aust. J. Chem. 25 (1972), 1565–1568.

[32] A. A. El-Asmy, O. A. El-Gammal, H. S. Saleh, Spectrochim. Acta Part A 71 (2008), 39–44.

[33] R. K. Tukhtaev, A. I. Gavrilov, Z. A. Saveljeva, S. V. Larionov, V. V. Boldyrev, J. Mater. Syn. Proc. 7 (1999), 19–22.

[34] P. S. Nair, G. D. Scholes, J. Mater. Chem. 16 (2006) 467–471.

[35] M. Mashima, Bull. Chem. Soc. Jpn. 37 (1964), 974–976.

[36] M. Haque, M. S. Hussain, Trans. Met. Chem. 19 (1994) 95–98.

[37] J. Park, E. Kang, S. U. Son, H. M. Park, M. K. Lee, J. Kim, K. W. Kim, H. Noh, J. Park, C. J. Bae, J-H. Park, T. Hyeon, Adv. Mater. 17 (2005), 429–434.

[38] R. Jenkins, R. L. Snyder, in: Chemical Analysis: Introduction to X-ray Powder Diffractometry, John Wiley & Sons, Inc., New York, 1996, p. 90

[39] M. Salavati-Niasari, F. Davar, M. Mazaheri, Mater. Res. Bull. 44 (2009), 2246–2251.

[40] M. Salavati-Niasari, Z. Fereshteh, F. Davar, J. Alloys Compd. 476 (2009), 797–801.

[41] M. Salavati-Niasari, F. Davar, Mater. Lett. 63 (2009), 441–443.

[42] P. S. Nair, T. Radhakrishnan, N. Revaprasadu, G. A. Kolawole, P. O'Brien, Polyhedron 22 (2003), 3129–3135.

[43] A. M. Qin, Y. P. Fang, W. X. Zhao, H. Q. Liu, C. Y. Su, J. Cryst. Growth 283 (2005), 230–241.

[44] Z. Fu, S. Zhou, J. Shi, S. Zhang, Mater. Res. Bull. 40 (2005), 1591–1598.